Polymer 50 (2009) 4334–4342

Contents lists available at ScienceDirect

Polymer

journal homepage: www.elsevier.com/locate/polymer

RAFT miniemulsion polymerization of methyl methacrylate

Lei Yang [b], Yingwu Luo [a,*], Xinzhi Liu [a], Bogeng Li [a]

[a] The State Key Laboratory of Chemical Engineering, Department of Chemical and Bio-Chemical Engineering, Zhejiang University, Hangzhou 310027, PR China
[b] Key laboratory of Advance Textile Materials and Manufacturing Technology, Ministry of Education, College of Materials and Textiles, Zhejiang Sci-Tech University, Hangzhou 310018, Zhejiang, PR China

ARTICLE INFO

Article history:
Received 26 March 2009
Received in revised form
23 June 2009
Accepted 1 July 2009
Available online 7 July 2009

Keywords:
RAFT polymerization
Miniemulsion polymerization
Methyl methacrylate

ABSTRACT

It has been well documented that RAFT miniemulsion polymerization has broader molecular weight distribution, compared with its bulk polymerization counterpart. Interestingly, it was found that the PDI value of RAFT miniemulsion polymerization of methyl methacrylate (MMA) mediated by 2-cyanoprop-2-yl dithiobenzoate (CPDB) was still as low as its corresponding bulk polymerization did. PDI could be as low as 1.13 even with typical sodium dodecyl sulfate (SDS, 1 wt%, surfactant) and *n*-hexadecane (HD, 2 wt%, costablizer) concentrations. When the polymerization was carried out at 60 °C, a dramatic increase in PDI (>1.4) was observed after 80% monomer conversion since RAFT addition reaction became diffusion-controlled. Increasing the polymerization temperature to 80 °C could reduce the PDI to 1.2 even at 100% monomer conversion. The compartmentalization effect of radicals was surprisingly absence before 30% monomer conversion but became pronounced afterwards in the miniemulsion polymerization. Thus, it still took less time to finish the miniemulsion polymerization with the increase of the surfactant levels.

1. Introduction

During the past decade, controlled/living radical polymerization (CLRP) was extensively investigated [1–3]. Three major CLRP methods, i.e. nitroxide-mediated polymerization (NMP) [4–7], atom transfer radical polymerization (ATRP) [8–11], and reversible addition-fragmentation chain transfer (RAFT) polymerization [12–18], demonstrated excellent control over the polymer chain microstructures and architectures. Well-defined (co)polymers with pre-determined molecular weights, narrow molecular weight distributions, pre-designed composition profiles and complex macromolecular architectures such as block, star, and comb copolymers were synthesized [13,14,19,20].

The RAFT polymerization can be carried out under the conditions similar to that of the conventional radical polymerization. Besides the components used in a conventional radical polymerization, a RAFT agent with a general structure S = C(Z) − SR is employed, where Z is the activating group and R is the leaving/re-initiating group [21,22]. The RAFT polymerization mechanism, as illustrated in Scheme 1, has been well accepted [23]. RAFT process (Reaction II or Reaction IV in Scheme 1) is a reversible transfer process in which free radicals react degeneratively with the dormant species (Species (2)). The irreversible termination (Reaction V) still occurs in the RAFT polymerization. In the RAFT bulk or solution polymerization, the irreversible termination is usually suppressed by using a low ratio of initiator to the RAFT agent concentrations. Thus, the polymerization rate becomes much lower than that of the regular (i.e. non-living) radical polymerization when the target molecular weight is high.

The RAFT miniemulsion polymerization of styrene was extensively investigated. Both the theoretical and experimental results demonstrated that the RAFT polymerization had a strong compartmentalization effect of radicals (i.e. the radical within a particle is physically isolated from the other one in the other particle), allowing to suppress the degree of the irreversible bi-radical termination at the little expense of the polymerization rate [24]. However, it was found that the RAFT miniemulsion polymerization was not as simple as adding the RAFT agent to the recipe of the regular miniemulsion polymerization. Actually, the early RAFT miniemulsion polymerization achieved few successes. In the most-investigated RAFT miniemulsion polymerization of styrene, the colloidal instability, as indicated by an oil layer separated from the emulsion system shortly after the initiation, poor control over molecular weights and very low polymerization rates were found [25–28]. Luo et al.'s simulations revealed the complex coupling phenomena of polymerization and monomer mass transfer among droplets/particles in the early stage of the polymerization [29]. Depending on the degree of monomer mass transfer, the colloidal system could lose stability or broaden molecular weight distribution and particle size

* Corresponding author. Tel.: +86 571 87951832; fax: +86 571 87951612.
E-mail address: yingwu.luo@zju.edu.cn (Y. Luo).

0032-3861/$ – see front matter © 2009 Elsevier Ltd. All rights reserved.
doi:10.1016/j.polymer.2009.07.002

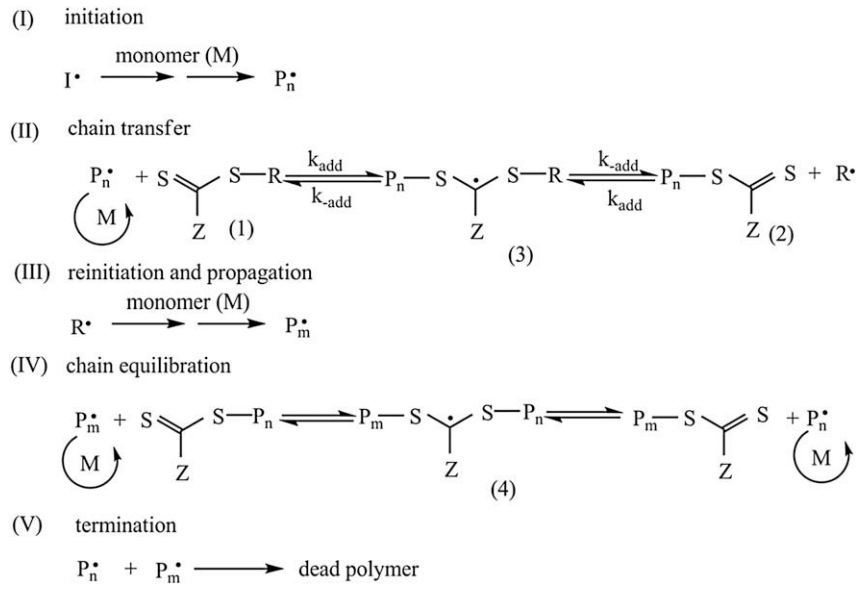

Scheme 1. Mechanism of RAFT polymerization [21].

distribution. Good colloidal stability could be achieved by using oligomers as a controlling/mediating agent [30], non-ionic polymeric surfactant [25], post addition of surfactant after emulsification process [31], and high levels of sodium dodecyl sulfate (SDS) and *n*-hexadecane (HD) [32,33] in the RAFT miniemulsion polymerization. However, it was well documented that the molecular weight distribution of RAFT miniemulsion polymerization was still broader than those of their homogeneous counterparts [31,33–35]. PDI was generally higher than 1.2 [31,33–35]. In the RAFT polymerization of styrene, PDI was found to dramatically increase with the increase of the targeted molecular weight [34]. In the aspect of polymerization rate, the number of particles of the RAFT miniemulsion polymerization was found far less than those of their regular miniemulsion polymerization counterparts [35]. For the zero-one kinetic systems like the (mini)emulsion polymerization of styrene with the particle diameter enough small, the average number of propagating radicals per particle was formulated as $\bar{n}^{-1} = \bar{n}_{\text{blank}}^{-1} + 2K[\text{RAFT}]$ [36]. Compared with styrene, the RAFT miniemulsion polymerization of butyl acrylate (BA) was more difficult to reach a low PDI value [37]. The PDI value was found to be significantly dependent on the type of RAFT agent. Only the RAFT agent with the primary R group and Z group with less stabilizing ability to the intermediate radicals was able to achieve a narrow molecular weight distribution and short inhibition period. Just like the styrene polymerization, the PDI values of the BA RAFT miniemulsion polymerization were also higher than those of their bulk counterparts [37].

The RAFT miniemulsion polymerization of methyl methacrylate, another typical monomer of radical polymerization, was much less studied. Zhou et al. [38] reported that the PDI values of RAFT MMA polymerization in miniemulsion could be decreased by using a small amount of β-cyclodextrin. It was assumed that β-cyclodextrin could help to transport the RAFT agent among particles and thus lead to the even distribution of RAFT agent among particles. Fundamentally, MMA (mini)emulsion polymerization is quite different from that of styrene [39,40]. Firstly, styrene (mini)emulsion polymerization follows a classic zero-one kinetic when the radii of particles are less than around 70 nm [40]. However, in MMA miniemulsion polymerization, it was suggested that radicals are not fully isolated within each particle.

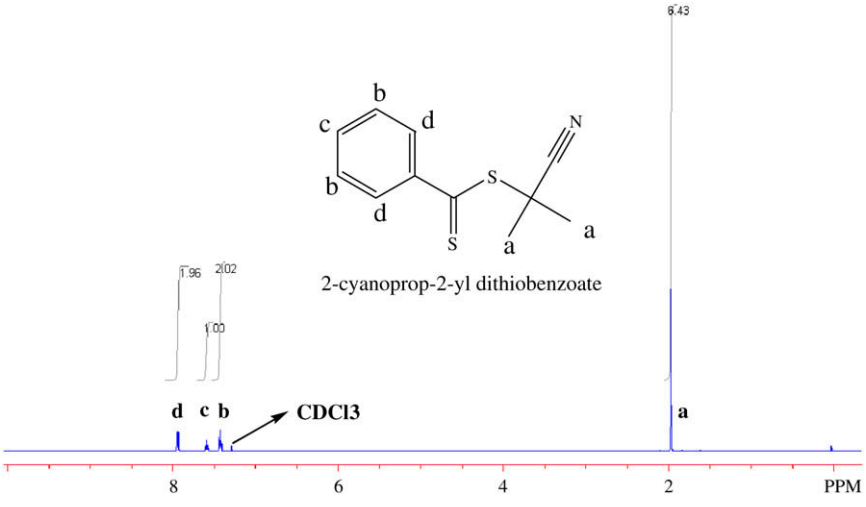

Fig. 1. ^{1}H NMR Spectrum of CPDB.

They actually are prone to exit and re-enter among different particles in the form of monomer radicals, resulting from the radical transfer reaction to monomer. The MMA (mini)emulsion polymerization was thought to follow pseudo-bulk kinetics. Secondly, the initiation efficiency of the water-soluble initiator is close to 1, much higher than that of styrene, due to the higher monomer solubility in water. Thirdly, the homogeneous nucleation is more likely to occur in the case of MMA. Fourthly, the gel effect of MMA polymerization is more profound. Thus, the investigation on MMA RAFT miniemulsion polymerization is greatly important both in academic and commercial applications. In this paper, a comparison study between MMA miniemulsion polymerization mediated by CPDB and its bulk counterpart as well as RAFT miniemulsion polymerization of styrene is conducted in terms of the kinetics and molecular weights and their distributions. The results will shed more insights on the RAFT miniemulsion polymerization.

2. The experimental

2.1. Materials

De-ionized water (conductivity < 4 μS/cm) was used as received. Methyl methacrylate (MMA) was purified by vacuum distillation. 2,2′-Azobis(isobutyronitrile) (AIBN, 98%) was re-crystallized twice from methanol. Potassium persulfate (KPS, >99%), sodium dodecyl sulfate (SDS, surfactant), hexadecane (HD, co-stabilizer, from Aldrich) were used without further purification. 2-Cyranoprop-2-yl dithiobenzoate (CPDB, RAFT agent) was synthesized and purified according to the reference [21,41]. The needle crystals of CPDB were collected. The purity of RAFT agent was highly pure as indicated by ^{1}H NMR (Fig. 1).

2.2. Batch miniemulsion polymerization

The miniemulsion was prepared according to the following procedure. MMA was first mixed with hexadecane and CPDB. This organic mixture was then added to the aqueous phase (water and SDS) under stirring. After 10 min, the formed coarse emulsion mixture was ultrasonified by using a KS-600 Sonifier (amplitude 70%, 600 W) for 15 min. The obtained miniemulsion was then transferred to a 250 ml five-neck flask reactor, equipped with a condenser, a thermometer, a nitrogen inlet, and a mechanical stirrer. The miniemulsion was aged at room temperature for 15 min. The reactor was immersed in a thermostated water bath at 60 °C (or 80 °C). Then the system (deoxygenated for 60 min before the miniemulsion was charged) was deoxygenated by purging with nitrogen for 15 min. Finally, the addition of KPS dissolved in 5 g water gave the zero time of the polymerization. The regular withdrawal of samples was separated into two parts. One was quenched with the hydroquinone ethanol solution. The other one was quenched with the hydroquinone SDS aqueous solution. This allowed us to follow the conversion of monomer as a function of time and the evolution of molecular weights and their distributions and particles sizes against monomer conversion.

2.3. Bulk polymerization

The mixture of MMA, AIBN and CPDB was transferred to glass tubes ($\Phi = 0.5$ cm) and deoxygenated by evacuating and re-filling with high pure nitrogen for five times. The tubes, sealed with septa, were then bathed in 60 °C water. A tube was removed at the pre-set time. The reactions were quenched by cooling the solutions in an ice bath and adding hydroquinone tetrahydrofuran (THF) solution. The polymer was isolated by evaporating off the solvent and residual monomer.

2.4. Characterization

Monomer conversion was followed gravimetrically. Molecular weight and its distributions of the polymers were determined at 30 °C by GPC (Waters 2487/630C) with three Polymer Laboratory columns (HR2, HR3 and HR4, the effective molecular weight range covers 500–600,000 g/mol for polystyrene) with a Refractive Index (RI) and UV dual detector system. The eluent was THF with a flow rate of 1 ml/min. The measurement was calibrated using narrow poly(methyl methacrylate) standards (Polymer Laboratory) with molecular weight ranging from 2580 to 981,000 g/mol. ^{1}H NMR spectra were measured (Internal reference: TMS (tetramethylsilane), 1% solution in CDCL3) on AVANCE DMX500. The samples for particle size analysis were first diluted with 50 parts of de-ionized water and then kept at 50 °C under vacuum overnight to drive off the residual MMA. The particle size was measured by a dynamic light scattering (Malvern 3000HSA) after a sonification treatment. The number of particles (N_P) was calculated by

$$N_P = \frac{6M_T x}{\pi \bar{d}_w^3 \rho_p} \quad (1)$$

3. Results and discussion

3.1. The influence of the heterogeneous nature on $\overline{M}_n$, PDI and polymerization kinetics

3.1.1. Molecular weight and its distribution

Table 1 summarizes the experimental recipes used in the current study as well as the resulted particle sizes and the number of particles. Expt 1–3 were carried out with the same RAFT concentrations. Expt 1 is a comparison experiment of the bulk polymerization. The typical SDS and HD concentrations for the conventional (non-"living") miniemulsion polymerization were employed in Expt 2. In Expt 3, both SDS and HD concentrations are higher than that in Expt 2, which was found to beneficial to stabilize the latex and to obtain the lower PDI value in our previous study of styrene [35]. It is worthy pointing out that the AIBN

Table 1
The experimental recipes and some analysis results.

Expt	MMA (g)	Water (g)	Initiator (g)	RAFT agent (g)	SDS (wt%)	HD (wt%)	$\bar{d}_w$ (nm)[a]	N_P (/ml H_2O)[a]
1[b]	20	–	0.035	0.23	–	–	–	–
2[b]	20	80	0.06	0.23	1	2	210	3.8×10^{13}
3[b]	20	80	0.06	0.23	5	5	120	2.3×10^{14}
4[b]	20	80	0.06	0.075	5	5	93	4.8×10^{14}
5[c]	20	80	0.06	0.29	5	5	89	6.8×10^{14}

[a] The data were acquired at 90%, 96%, 95% and 100% conversion for Expt 2–4 respectively.
[b] Experiments were carried out at 60 °C.
[c] Experiment was carried out at 80 °C.

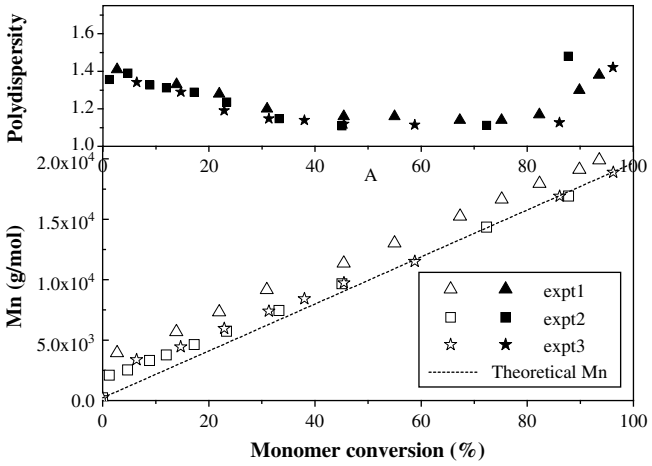

Fig. 2. Mn and PDI versus conversion for Expt 1–3.

concentration of Expt 1 was set so that the initiation rate of Expt 1 was close to that of the miniemulsion polymerization, where KPS was used as initiator.

In Expt 2, the minor oil bulk phase was observed after the injection of the initiator (KPS) aqueous solution, but it disappeared shortly after 5% monomer conversion. The latex then remained stable. Clearly, the system was more stable than the styrene one, where the sticky aggregates were obtained in the end of the polymerization under the similar conditions [35]. No colloidal instability issues were found in Expt 3 as a result of higher SDS and HD concentrations, which is in accord with the case of styrene.

Fig. 2 represents the plots of $\overline{M}_n$ and PDI values against monomer conversions in the bulk (Expt 1) and miniemulsion polymerizations (Expt 2 and 3). The theoretical $\overline{M}_n$ s were calculated from Eq. (2) [25–27].

$$\overline{M}_n = M_{\mathrm{RAFT}} + \frac{x[M]_0 M_M}{[\mathrm{RAFT}]_0 + 2f[I]_0(1-e^{-k_d t})} \tag{2}$$

From Fig. 2, the followings are derived:

A. $\overline{M}_n$ s of three experiments increase linearly with conversion. $\overline{M}_n$ s deviate a little from the theoretical lines in the early stage. After 30% monomer conversion, $\overline{M}_n$ s become in good agreement with those theoretical values in Expt 2 and 3. $\overline{M}_n$ s of Expt 1 are a little higher than those of Expt 2 and 3 during the whole conversion range probably due to the experimental errors.

B. PDI changing trends are almost overlapped before 70% monomer conversion. PDI decreases from around 1.4 and then levels off at 1.11 after 30% conversion. Three samples with very close $\overline{M}_n$ values were selected from Expt 1–3 and their GPC spectra are compared in Fig. 3. Three curves are completely overlapped. It is evident that the nano-heterogeneous nature of the miniemulsion polymerization has no effect on the molecular weight distribution in this system. That is, each particle produces polymer chains with the same molecular weight. This observation is quite different from the case of styrene and butyl acrylate, where the PDI was found to be higher in the RAFT miniemulsion polymerization than their bulk counterparts and was significantly dependent on the recipe of the miniemulsion polymerization [35,37].

C. After 70–80% monomer conversion, PDI dramatically increases but with different rates for three polymerization runs. As a comparison, PDI did not increase in the late stage of styrene RAFT polymerization [31,34,35]. In Expt 1 and 2, PDI starts to increase after 70% conversion. The increase of PDI occurs much later at around 83% in Expt 3. The GPC curves before and after PDI increase are compared in Fig. 4. From Fig. 4, it is clear that a shoulder peak of higher molecular weight appears in the GPC spectra of the high conversion samples, contributing to the broadening of molecular weight distributions. Fig. 4 discloses that most of polymer chains stopped growing in the late stage of the polymerization.

As demonstrated by the simulations, the fraction of dead polymer could dramatically increase in the late stage of RAFT polymerization [42]. However, in the current study, the PDI increase in the late stage of the polymerization should not be caused by the irreversible termination. All the dormant chains derived from the RAFT agent (CPDB) own a benzene ring, which the dead polymer chains do not have. The polymer samples were analyzed with a GPC system with RI-UV dual detectors (the wave length of UV detector was set at 254 nm, where benzene rings show characteristic absorption). RI signal represented the contributions both from dormant and dead chains whereas only the dormant chains with benzene ring (from CPDB) contributed to UV signals. As compared Fig. 5 with Fig. 4, the UV spectra are in good agreement with the RI spectra, indicating the chains contributing to the shoulder peaks are also the dormant chains (note: the low elution time corresponds to the high molecular weight). They did not come from the irreversible termination. Additionally, the dominant termination mode for MMA polymerization is disproportional [43]. That means the higher molecular weight could not be the dead chains from the termination.

Zhu studied the effect of gel effect on RAFT polymerization by the simulations [42]. It was concluded that the chain length distributions could be broadened when the RAFT addition became diffusion-controlled. Butté studied the gel effect in MMA RAFT bulk polymerization mediated by cumyl dithiobenzoate at 70 °C [44]. Both the experimental and simulation results showed that the bimolecular termination as well as RAFT addition reactions became diffusion-controlled above 60% conversion. The PDI leveled off and then increased after 60% conversion. Very recent work by John-Hall et al. examined the chain length dependent termination rate coefficient in MMA RAFT polymerization [45–48]. In the late stage of the RAFT polymerization, the RAFT addition reactions, similar to the irreversible termination, involving two chains of high degree of polymerization, could become diffusion-controlled [42]. This can lead to a sharp decrease in the transfer constant ($C_{\mathrm{tr}} = 2k_{\mathrm{add}}/k_{\mathrm{p}}$) since the propagation rate constant would be less affected by the

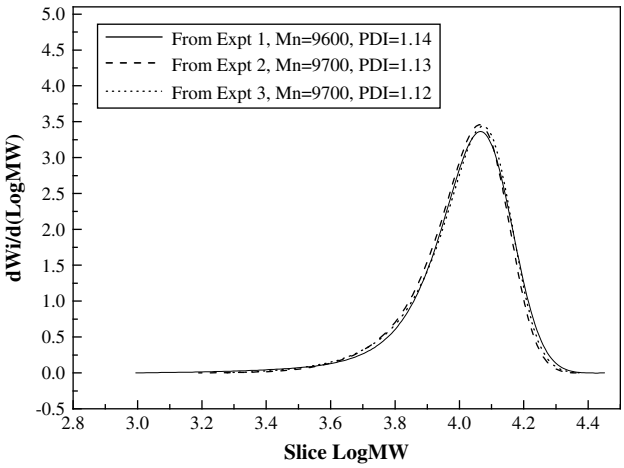

Fig. 3. Comparison of GPC curves from the samples with close molecular weight in Expt 1–3.

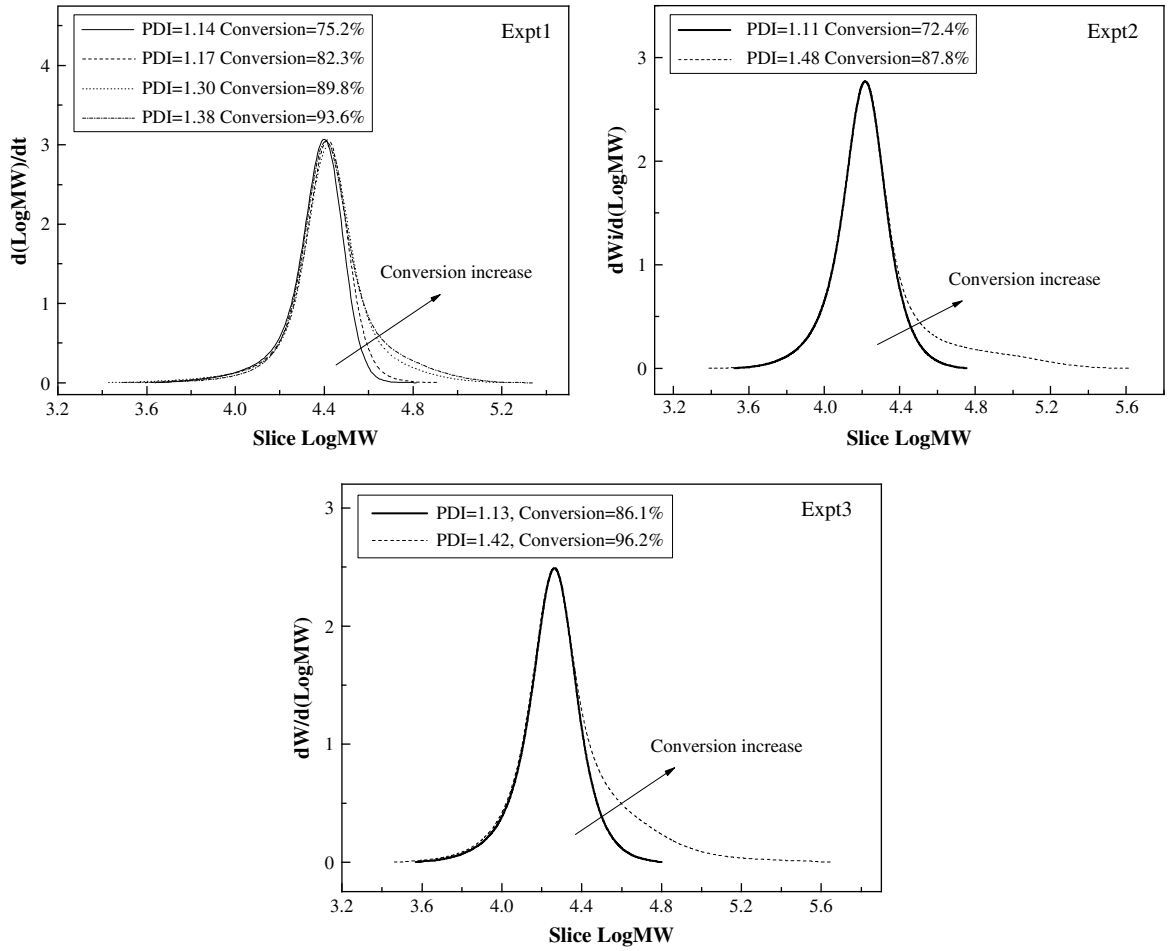

Fig. 4. Comparison of GPC curves of Expt 1–3, scaled with conversion.

reactant diffusion [49]. This is the main reason for the increases of PDI observed in the late stage of Expt 1–3.

Generally speaking, the conversion where the RAFT addition reaction becomes diffusion-controlled should be the same in the solvent free polymerization like bulk and miniemulsion polymerizations as targeting at the same molecular weight. However, (mini)-emulsion polymerization could have some kind of plasticization effect [39]. That is why the PDIs of Expt 3 started to increase after 83% conversion, much later than in Expt 1. In Expt 2, the plasticization effect is much weakened due to the larger particle size of 210 nm, so the changing trend of PDI is similar to that of Expt 1. The changing trends of the PDI with the particle sizes are in accordance with the observation of the limiting conversion as discussed later.

3.1.2. Polymerization kinetics

3.1.2.1. Polymerization rates and limiting conversion. Fig. 6 presents the conversion-time plots of all polymerization runs. The most striking observation is that the kinetic curves of Expt 1–3 are nearly overlapped before 30% monomer conversion. Because the initiation rate ($R_i = 2fk_d[I]$, refer to nomenclature for the values of each parameter) in Expt 1–3 were close to each other as designed, it is suggested that the radical isolation effects, which observed in styrene RAFT miniemulsion polymerization, are actually absence in the current systems. A closer examination reveals that in the beginning (see the inlet of Fig. 6), the polymerization rates of the miniemulsion polymerization (Expt 2 and 3) are even a little lower than that in the bulk polymerization. After 30% conversion, the polymerization rates increase with the decrease of the particle size (refer to Table 1 for particle size and the particle size in the bulk polymerization could be considered to be infinite). The profound isolation effect of radicals is clearly seen. As a result, it took 455 and 351 min for Expt 2 and 3 to reach 85% conversion, respectively, which were much shorter than 710 min in the bulk polymerization (Expt 1).

Due to the relatively high monomer transfer constant and relatively high water solubility of monomer, radicals within particles could transport frequently in the form of monomer radicals among different particles in the emulsion polymerization of MMA [39]. This means the isolation effect of radicals in (mini)emulsion would be weakened [39]. It was suggested that the regular emulsion polymerization of MMA should follow pseudo-bulk polymerization kinetics, instead of the classic zero-one kinetics [39]. The radical exchange among particles would be more pronounced in the early stage of RAFT miniemulsion polymerization [50]. In Expt 2 and 3, CPDB with a *R* group of $CN(CH_3)_2C$was employed as the RAFT agent. Since the transfer constant of the RAFT agent is rather high (for CPDB, $C_{tr} = 13$) [51], the radicals within a particle could quickly convert into the small radicals of the leaving group (for CPDB, $CN(CH_3)_2C^{\cdot}$). Just like the monomer radicals, these small radicals could exit out of the particle and re-enter other particles. Thus, the radical within a particle is very movable among particles, leading to the disappearance of the radical isolation effect. As a result, the kinetics of RAFT miniemulsion polymerization of MMA is just the same as that of the bulk polymerization if the termination of radicals in the water is negligible when the conversion was lower than 30%. When the monomer conversion was higher than 30%, the RAFT miniemulsion polymerization showed a polymerization

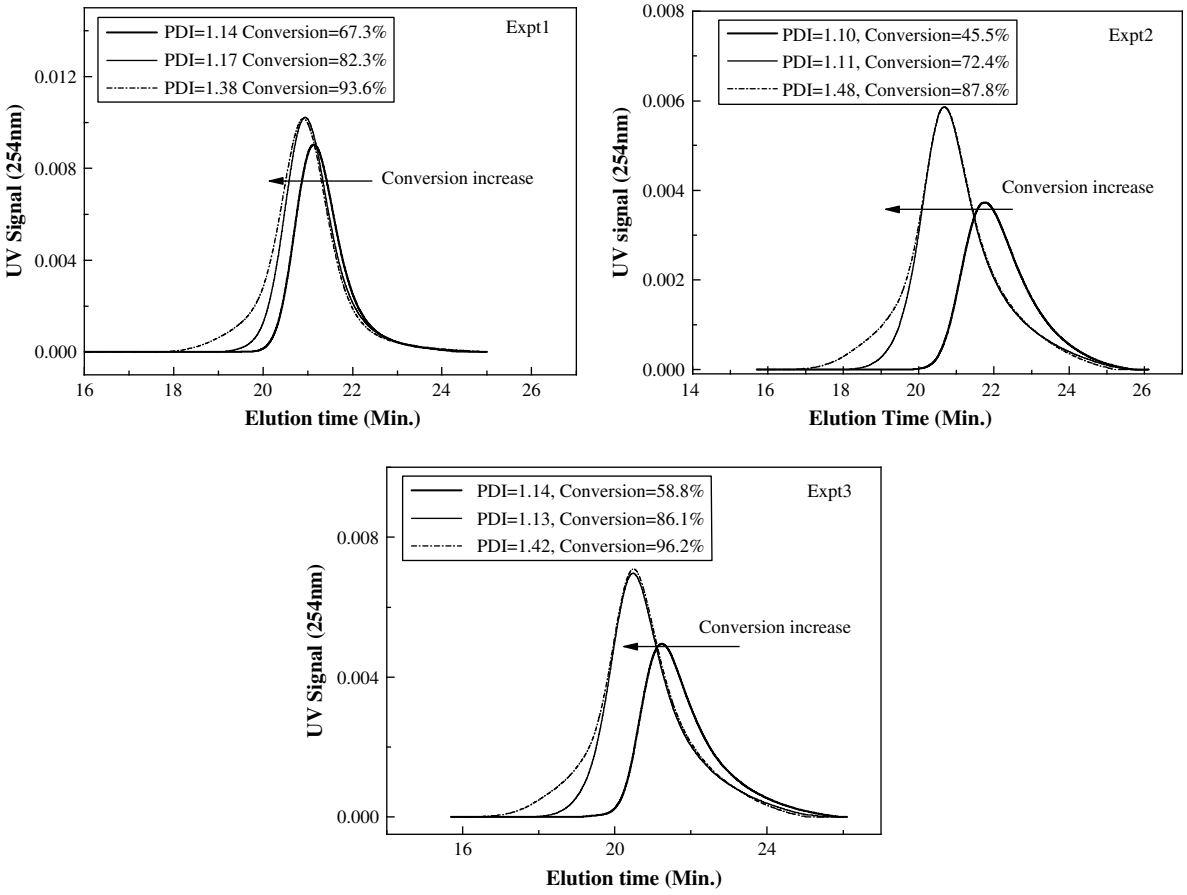

Fig. 5. UV signal GPC curves of Expt 1–3, scaled with conversion.

enhancement due to the decrease of particle sizes, as seen in Fig. 6. This could be ascribed to two reasons. On the one hand, CPDB molecules were fully converted into polymer dormant chains and thus the CPDB induced radical exit disappeared. On the other hand, the exit rate of monomer radicals might also be reduced because of the high viscosity within particles.

In the radical polymerization, the monomer conversion could be nearly stopped by the so-called glass effect when the glass transition temperature (T_g) of the system became close to the polymerization temperature [52]. The limiting conversion of MMA bulk polymerization at 60 °C was estimated to be 85% from the free volume theory (Eq. (3)) [53] by setting T_g to be the polymerization temperature.

$$T_g = \frac{\alpha_1(1-\phi_2)T_{g1} + \alpha_2\phi_2 T_{g2}}{\alpha_1(1-\phi_2) + \alpha_2\phi_2} \quad (3)$$

The limiting conversions were observed in Expt 1–3. As seen in Fig. 6, the limiting conversion of Expt 3 is higher than those of Expt 1 and 2 because of the plasticization effect of (mini)emulsion systems. Similar results was reported in the nonliving emulsion polymerization systems [39].

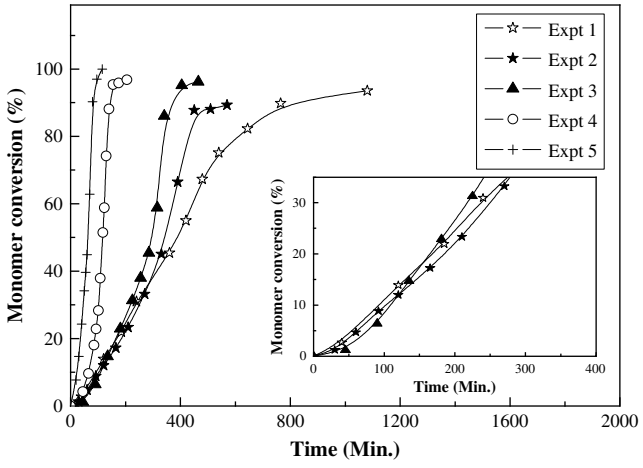

Fig. 6. Conversion versus time curves for Expt 1–5.

3.1.2.2. Evolution of N_P against monomer conversion. The evolution of the particle sizes was monitored during the polymerization in Expt 2 and 3. Combining the kinetic curves in Fig. 6, the evolution of N_P against conversion was plotted, as shown in Fig. 7.

From Fig. 7, the nucleation process of RAFT miniemulsion polymerization with respect to monomer conversion seems to be similar to that of non-RAFT miniemulsion polymerization, but the RAFT systems end with the much lower number of particles than their regular miniemulsion polymerization counterparts [54]. Furthermore, the final N_P increases with decrease of RAFT concentrations and increase of the polymerization temperature. The low number of particles means the low nucleation efficiency of monomer droplets, probably resulted from the superswelling of the particles in the very beginning of the polymerization. These features were also observed in the RAFT miniemulsion polymerizations of other monomers [35].

3.1.2.3. The average number of propagating radicals per particle ($\bar{n}$). The $\bar{n}$ s of Expt 2 and 3 were calculated via Eq. (4) from, the

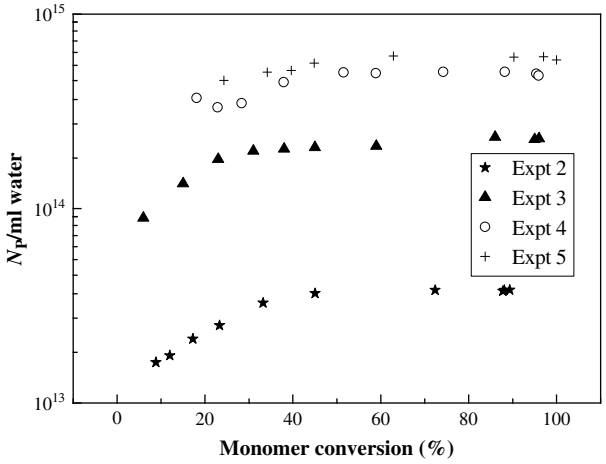

Fig. 7. N_P changing trends with monomer conversion in Expt 2–5.

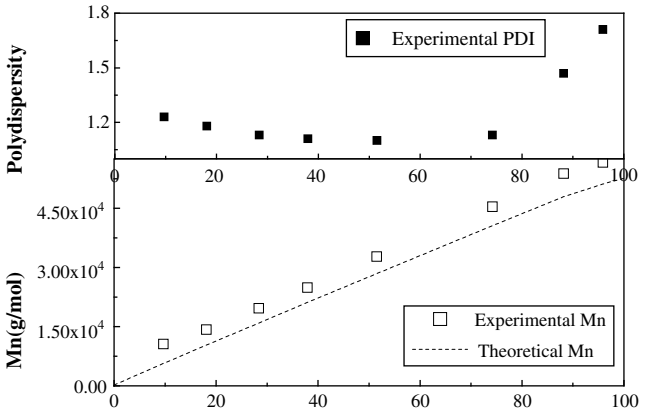

Fig. 9. Mn and PDI changing trends with conversion for Expt 4 targeting to higher molecular weight.

kinetics and N_P as presented in Figs. 6 and 7, respectively. The evolution of $\overline{n}$ with conversion is shown in Fig. 8.

$$\overline{n} = \frac{\left(-\frac{d[M]_P}{dt}\right)N_A}{k_P[M]_P N_P} \quad (4)$$

The $\overline{n}$ in Expt 2 before 35% conversion holds at about 0.2. It starts to increase sharply after 35% conversion. The similar changing trend of $\overline{n}$ is seen in Expt 3. This could be ascribed to that the radical exit becomes more difficult after 35%, as discussed previously. In the stage of the high conversion (>60%), the gel effect might also contribute to $\overline{n}$ increase. The $\overline{n}$ before 40% conversion is only about 0.03 in Expt 3. The very low $\overline{n}$ is partly due to the RAFT retardation [36] and partly due to no isolation effect of radicals discussed above.

3.2. Synthesis of poly(methyl methacrylate) with higher molecular weight

In styrene [34] miniemulsion polymerization mediated by RAFT, the PDI increased significantly with increase of the targeting $\overline{M}_n$ [32]. It was difficult to synthesize polystyrene of high molecular weight (>5.0×10^4 g/mol) with low PDI (<1.5) in the batch miniemulsion polymerization [34]. In Expt 4, as shown in Fig. 9, the targeted $\overline{M}_n$ of PMMA was increased to 5.9×10^4 g/mol. Contrary to the situations of the styrene [34] miniemulsion polymerization, the higher targeted molecular weight does not increase the PDI of the product. The PDIs of PMMA in Expt 4 remain below 1.20 till 75% conversion, which is comparable with the data with higher levels of the RAFT agent (Expt 2 and 3). To synthesis polystyrene of such high molecular weight, the PDIs were as high as about 1.5 throughout the polymerization [34]. The PDI in the late stage of Expt 4 dramatically increases and reaches 1.71 at 96% conversion since the RAFT addition reaction becomes diffusion-controlled as discussed above. It is clear that the diffusion effect on PDI values is more pronounced when targeting at the higher molecular weight.

As seen in Fig. 6, the retardation in polymerization rate is relieved when the concentration of the RAFT agent is reduced (i.e. increasing the target molecular weight). Compared with Expt 2–3, the polymerization rate increases remarkably in Expt 4. It took only 140 min to reach 85% conversion. The increase in both $\overline{n}$ as evidenced in Fig. 8 and N_P as evidenced in Fig. 7 contributes to the increase of the polymerization rate in Expt 4. Similar phenomena were observed in the RAFT miniemulsion polymerization of styrene [35].

3.3. Miniemulsion polymerization at higher temperature

In Expt 5, the reaction temperature was increased to 80 °C in order to weaken the influence of the gel effect on RAFT reactions and to relieve of the glass effect. The kinetic curve was shown in Fig. 6. The data of $\overline{M}_n$ and PDI against conversion are presented in Fig. 10.

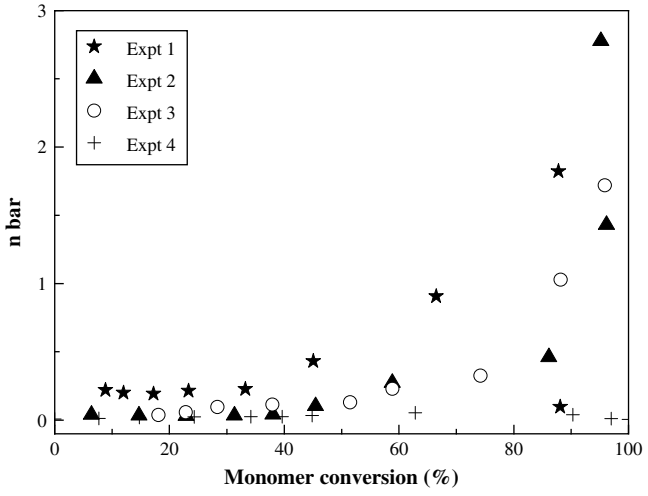

Fig. 8. Changing trends of n bar with monomer conversion in Expt 2–5.

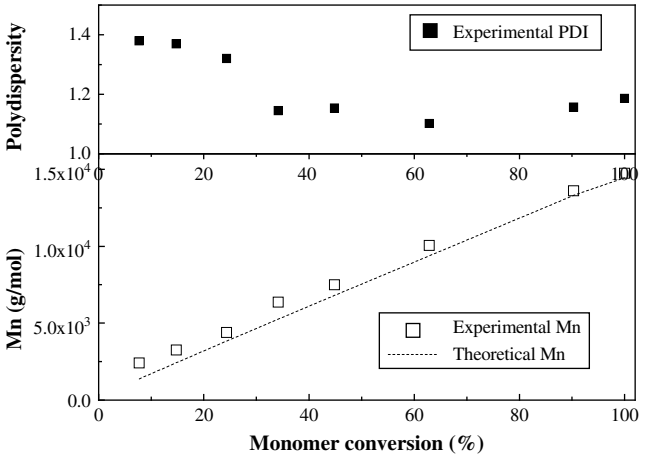

Fig. 10. Mn and PDI changing trends with conversion for Expt 5 run at 80 °C.

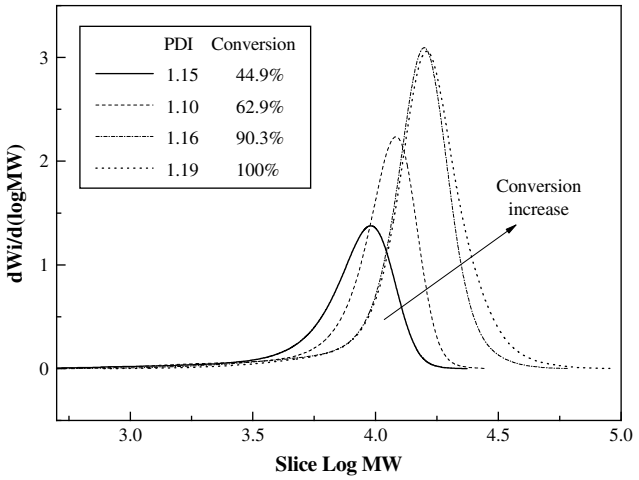

Fig. 11. GPC curves for Expt 5 carried out at 80 °C.

In Fig. 10, $\overline{M}_n$ s grow linearly with conversion and agree well with the theoretical ones. The colloidal stability was excellent. The PDIs remain below 1.20 during the entire conversion range. Though the shoulder peak is still seen in the GPC curve at conversion 100% as seen in Fig. 11, it is much less obvious in Expt 5 due to a weakened gel and glass effect.

As the reaction temperature increases, both N_P and the propagation rate constant increase. The polymerization proceeded at a much higher rate and the full conversion was achieved after 115 min. No limit conversion was found any more, as seen in Fig. 6. As compared with Expt 3, $\overline{n}$ of Expt 5 is a little lower. The increase in $\overline{n}$ is also observed in the middle stage of the polymerization. However, it is greatly weakened. These findings are in accordance with the weakened gel and glass effects.

4. Conclusion

4.1. With regard to the MMA miniemulsion polymerizations mediated by CPDB, the following conclusions are drawn

- With 1 wt% SDS and 2 wt% HD concentrations, the colloidal systems still remained stable.
- The molecular weight distribution was comparable to that of the bulk polymerization with PDI lower than 1.2.
- Compartmentalization effect of radicals was not observed before 30% monomer conversion but it became pronounced later on. One could much shorten the polymerization time by using miniemulsion polymerization technique.
- At 60 °C, RAFT addition reaction became diffusion-controlled after 80% monomer conversion, leading to a dramatic increase in PDI. PDI started to increase later in the miniemulsion polymerization than in the bulk polymerization. Increasing the polymerization temperature to 80 °C could reduce the PDI to 1.2 even at 100% conversion.
- The PDI value was little affected by the targeting molecular weight (up to 59,000 g/mol).
- With increase of RAFT concentrations, N_P value decreased, indicating that the droplet nucleation efficiency was lowered.

With exception of the last point, all the observations above are quite different from the RAFT miniemulsion polymerization of styrene. To our best knowledge, this work demonstrated, for the first time, that not only could RAFT miniemulsion polymerization much increase the polymerization rate but also remain the same controlling degree over molecular weight and its distribution, as compared with the corresponding bulk polymerization. We believe that the narrow molecular weight distributions comparable to the bulk polymerization should be related to the absence of the compartmentalization effect of radicals in the early stage of MMA RAFT miniemulsion polymerization. The occurrence of the compartmentalization effect led to the increase in the polymerization rate after the middle stage of the miniemulsion polymerization.

Acknowledgement

This project is financially supported by NSF of China (Grant No. 20204015, 20474057, 20836007), Zhejiang Provincial Natural Science Foundation of China (Y4080375), Science Foundation of Zhejiang Sci-Tech University (ZSTU, 0701065–Y), and Program for New Century Excellent Talents in University.

References

[1] Qiu J, Charleux B, Matyjaszewski K. Prog Polym Sci 2001;26:2083.
[2] Cunningham MF. Prog Polym Sci 2002;27:1039.
[3] Davis KA, Matyjaszewski K. Adv Polym Sci 2002;159:1.
[4] Georges MK, Veregin RPN, Kazmaier PM, Hamer GK. Macromolecules 1993; 26:2987.
[5] Moad G, Rizzardo E, Solomon DH. Macromolecules 1982;15:909.
[6] Hawker CJ, Bosman AW, Harth E. Chem Rev 2001;101:3661.
[7] Solomon DH. J Polym Sci Part A Polym Chem 2005;43:5748.
[8] Kato M, Kamigaito M, Sawamoto M, Higashimura T. Macromolecules 1995;28:1721.
[9] Matyjaszewski K, Gaynor S, Wang JS. Macromolecules 1995;28:2093.
[10] Matyjaszewski K, Xia JH. Chem Rev 2001;101:2921.
[11] Kamigaito M, Ando T, Sawamoto M. Chem Rev 2001;101:3689.
[12] Moad G, Chong YK, Postma A, Rizzardo E, Thang SH. Polymer 2005;46:8458.
[13] Moad G, Rizzardo E, Thang SH. Aust J Chem 2005;58:379.
[14] Perrier S, Takolpuckdee P. J Polym Sci Part A Polym Chem 2005;43:5347.
[15] Barner-Kowollik C, Buback M, Charleux B, Coote ML, Fukuda T, Goto A, et al. J Polym Sci Part A Polym Chem 2006;44:5809.
[16] Moad G, Rizzardo E, Thang SH. Aust J Chem 2006;59:669.
[17] Favier A, Charreyre MT. Macromol Rapid Commun 2006;27:653.
[18] Barner-Kowollik C, Perrier S. J Polym Sci Part A Polym Chem 2008;46:5715.
[19] Braunecker WA, Matyjaszewski K. Prog Polym Sci 2007;32:93.
[20] Sheiko SS, Sumerlin BS, Matyjaszewski K. Prog Polym Sci 2008;33:759.
[21] Chong YK, Krstina J, Le TPT, Moad G, Postma A, Rizzardo E, et al. Macromolecules 2003;36:2256.
[22] Chiefari J, Mayadunne RTA, Moad CL, Moad G, Rizzardo E, Postma A, et al. Macromolecules 2003;36:2273.
[23] Chiefari J, Chong YK, Ercole F, Krstina J, Jeffery J, Le TPT, et al. Macromolecules 1998;31:5559.
[24] Butté A, Storti G, Morbidelli M. Macromolecules 2001;34:5885.
[25] Brouwer H, Monteiro MJ, German AL, Tsavalas JG, Schork FJ. Macromolecules 2000;33:9239.
[26] Tsavalas JG, Schork FJ, de Brouwer H, Monteiro MJ. Macromolecules 2000;33:9239.
[27] Lansalot M, Davis TP, Heuts JPA. Macromolecules 2002;35:7582.
[28] Monteiro MJ, Hodgson M, de Brouwer JAM. J Polym Sci Part A Polym Chem 2000;38:3864.
[29] Luo YW, Tsavalas J, Schork FJ. Macromolecules 2001;34:5501.
[30] Vosloo JJ, De Wet-Roos D, Tonge MP, Sanderson RD. Macromolecules 2002; 35:4894.
[31] Yang L, Luo YW, Li BG. J Polym Sci Part A Polym Chem 2006;44:2293.
[32] Tonge MP, McLeary JB, Vosloo JJ, Sanderson RD. Macromol Symp 2003;193:289.
[33] Yang L, Luo YW, Li BG. Acta Polym Sinica 2004;3:462.
[34] Yang L, Luo YW, Li BG. J Polym Sci Part A Polym Chem 2005;43:4972.
[35] Yang L, Luo YW, Li BG. Polymer 2006;47:751.
[36] Luo YW, Wang R, Yang L, Yu B, Li BG, Zhu SP. Macromolecules 2006;39:1328.
[37] Luo YW, Liu B, Wang ZH, Gao J, Li BG. J Polym Sci Part A Polym Chem 2007; 45:2304.
[38] Zhou XD, Ni PH, Yu ZQ. Polymer 2007;48:6262.
[39] Gilbert RG. Emulsion polymerization: a mechanistic approach. London: Academic; 1995.
[40] van Herk AM. Chemistry and technology of emulsion polymerization. Blackwell Publishing; 2005.
[41] Moad G, Chiefari J, Krstina J, Postma A, Mayadunne RTA, Rizzardo E, Thang SH. Polym Int 2000;49:933.
[42] Wang AR, Zhu SP. Macromol Theory Simul 2003;12:196.
[43] Zammit MD, Davis TP, Haddleton DM, Suddaby KG. Macromolecules 1997; 30:1915.
[44] Peklak DA, Butté A, Storti G, Morbidelli M. J Polym Sci Part A Polym Chem 2006;44:1071.

[45] John-Hall G, Theis A, Monteiro MJ, Davis TP, Stenzel MH, Barner-Kowollik C. Macromol Chem Phys 2005;206:2047.
[46] John-Hall G, Stenzel MH, Davis TP, Barner-Kowollik C, Monteiro MJ. Macromolecules 2007;40:2730.
[47] John-Hall G, Monteiro MJ. Macromolecules 2007;40:7171.
[48] John-Hall G, Monteiro MJ. J Polym Sci Part A Polym Chem 2008;46:3155.
[49] Matyjaszewski K, Davis TP. Handbook of radical polymerization. John Wiley and Sons, Inc.; 2002.
[50] Luo YW, Yu B. Polym Plast Tech Eng 2004;43:1299.
[51] Moad G, Chiefari J, Chong YK, Krstina J, Mayadunne RTA, Postma A, et al. Polymer Int 2000;49:993.
[52] Horie K, Mita I, Kambe H. J Polym Sci 1968;6:2663.
[53] Kelley FN, Bueche F. J Polym Sci 1961;50:549.
[54] Fontenot K, Schork FJ. J Appl Polym Sci 1993;49:633.
[55] Brandrup J, Immergut EH, Grulke EA. Polymer handbook. 4th ed. 1999. ISBN 0-471-16628-6).
[56] Faldi A, Tirrell M, Lodge TP, von Meerwall E. Macromolecules 1994;27:4184.

Nomenclature

$\bar{d}_w$: the volume-average diameter;
f : initiation efficiency, $f = 0.4$ in Expt 1. In Expt 2–5, $f = 0.65$, taking into account both the efficiencies for the conversion of initiator radicals to monomer and the radical entry into the particles (or droplets);
$[I]$: initiator concentration;
$[I]_0$: initial initiator concentration;
k_{add} : rate constant of free radical addition to the RAFT agent;
k_d : initiator decomposition rate constant. $k_d = 7.2 \times 10^{-4}\ s^{-1}$ for AIBN at 60 °C; $k_d = 1.64 \times 10^{-3}\ s^{-1}$ calculated from $k_d = 8.0 \times 10^{15} e^{[-124{,}500/RT]}\ s^{-1}$ in Expt 2–4[55]
k_P : monomer propagation rate constant. In Expt 1–4, $k_P = 1022$ l/mol/s before 84% conversion, $k_P = 1022 e^{[-29.8(x-0.84)]}$ l/mol/s when conversion exceeds 84%. In Expt 5, $k_P = 1590$ l/mol/s[55]
K : RAFT equilibrium constant;
M_T : initial monomer concentration in g_{MMA}/L_{water};
$\overline{M}_n$: the number average molecular weight of the polymer;
M_{RAFT} : the molar weight of CPDB, 221.3 g/mol;
M_M : the molar weight of MMA, 100.1 g/mol;
$[M]_0$: initial monomer concentration;
$[M]_P$: monomer concentration in the particles;
$\overline{n}$: number of radicals per particle;
N_A : Avogadro's number;
N_P : number of particles per liter of water;
$[RAFT]$: RAFT agent concentration;
t : polyreaction time, s;
T_{g1} : the glass transition temperature of MMA, 143 K[56]
T_{g2} : the glass transition temperature of PMMA, 392 K[56]
T_g : the glass transition temperature of mixture of MMA with PMMA;
x : monomer conversion;

Greeks

α_1 : differences between the thermal expansion coefficients above and below the glass transition temperature of MMA, $5.76 \times 10^{-4}\ K^{-1}$[56]
α_2 : differences between the thermal expansion coefficients above and below the glass transition temperature of PMMA, $3.21 \times 10^{-4}\ K^{-1}$[56]
ρ_P : density of PMMA, 1.19 g/ml;
ϕ_2 : the polymer volume fraction;

Subscripts

blank: RAFT-free miniemulsion polymerization system.